Proceedings of the ASME 2010 3rd Joint US-European Fluids Engineering Summer Meeting and 8th International Conference on Nanochannels, Microchannels, and Minichannels
FEDSM-ICNMM2010
August 1-5, 2010, Montreal, Canada

FEDSM-ICNMM2010-30288

ADVANCES IN DESIGN METHODS AND CHARACTERISTICS OF INTERNAL FLOW FOR CENTRIFUGAL PUMPS

YUAN Shouqi
Research Center of Fluid Machinery Engineering and Technology, Jiangsu University
Zhenjiang, Jiangsu, China
shouqiy@ujs.edu.cn

YUAN Jianping
Research Center of Fluid Machinery Engineering and Technology, Jiangsu University
Zhenjiang, Jiangsu, China
yh@ujs.edu.cn

LIU Houlin
Research Center of Fluid Machinery Engineering and Technology, Jiangsu University
Zhenjiang, Jiangsu, China
liuhoulin@ujs.edu.cn

TANG Yue
Research Center of Fluid Machinery Engineering and Technology, Jiangsu University
Zhenjiang, Jiangsu, China
tomt@ujs.edu.cn

ZHANG Jinfeng
Research Center of Fluid Machinery Engineering and Technology, Jiangsu University
Zhenjiang, Jiangsu, China
zhangjinfeng@ujs.edu.cn

PEI Ji
Research Center of Fluid Machinery Engineering and Technology, Jiangsu University
Zhenjiang, Jiangsu, China
craig.j.pei@gmail.com

ABSTRACT

Centrifugal pump is widely used in various fields of the national economy. Pumps, of which 70% are centrifugal pumps, consume 20.9% of the total electricity generation nationwide in China in 2009, according to the statistics. In this paper, the research advances in design methods and characteristics of internal flow fields for centrifugal pumps, carried out by the Research Center of Fluid Machinery Engineering and Technology of Jiangsu University, is introduced.

First of all, the Greater Flow Design method, Non-Overload Design method and Splitter Blade Offset Design method are fully discussed through systematically studies. In addition, three methods of performance prediction for centrifugal pumps are adopted, and a CAD/CFD software for hydraulic design and analysis is initially developed.

Secondly, to deepen the understanding of characteristics of internal flow in centrifugal pumps, the numerical simulation and PIV measurement investigation have been done. Then the unsteady flow induced vibration and noise are studied considering fluid-structure interaction and fluid-sound interaction. The control of the unsteady flow in centrifugal pumps is also attempted to optimize the design method for centrifugal pumps. In addition, the pressure pulsation and vibration behaviors under both cavitation and non-cavitation conditions are obtained and analyzed. Finally, some detecting methods and criterion for cavitation incipiency and development are put forward.

Keywords: Centrifugal pump, design method, unsteady flow characteristics, performance prediction, cavitation, FSI

NOMENCLATURE

H	head, m
Q	flow rate, m^3/h
P	horsepower, kW
n	speed of rotation, rpm
n_s	specific speed
Z	number of blades
β	blade angle, º
Φ	wrap angle of blade, º
D	diameter, mm
b_2	impeller outlet width, mm
d_h	impeller hub plate diameter, mm
ρ	density of water, kg/m^3
g	gravity accelerate, m/s^2
b_3	volute inlet width, mm
φ_0	tongue angle of volute, º
η	pump efficiency, %
η_h	hydraulic efficiency, %
η_v	volumetric efficiency, %
η_m	mechanical efficiency, %
w	relative velocity of flow, m/s

Subscript

1	inlet of impeller
2	outlet of impeller
3	inlet of volute
t	theoretical or volute tongue

0 INTRODUCTION

Energy is a generally concerned issue in the present-day world. Energy saving is not only a long-term strategy for the social and economic development in China, but also an extremely urgent mission at present. Pump, an important energy conversion and fluid transportation device, consumes about 20.9% of the total generated energy nationwide in China with a huge energy saving space. China has put forward the goal that unit GDP energy consumption will reduce by approximately 20% during the period of "the Eleventh Five-Year Plan", and pump has been listed in the plan as an important energy saving device. Centrifugal pump, as the most extensively applied pump machinery accounting for about 70% of pump machinery, is widely used in almost every department on national economy: aerospace, nuclear industry, agricultural irrigation, urban water supply, petroleum, chemistry and electric power, etc.

The overall technical level of pump industry in China is lagging behind the international level and other relative industries. In the past 20 years, the team led by the author of this paper engaged in long term the research on design methods, the patterns of internal flow, and energy saving technologies for system engineering of centrifugal pumps, etc.

This paper aims at comprehensively summarizing our research advances. First of all, our research on design method for centrifugal pumps and relevant results obtained, including the design method for low specific speed pumps, the design method for double channel pumps and CAD/CFD integrated software for centrifugal pumps, etc, are briefly introduced. Then the studies and relevant achievements concerning the characteristics of internal unsteady flow in centrifugal pumps, involving steady and unsteady numerical simulations for turbulent flow in centrifugal pumps, PIV measurement of inner flow fields, unsteady flow induced noise and vibration and FSI effect of centrifugal pumps, are summarized. Finally, the paper will look ahead our research work, such as study on design method for low vibration and low noise centrifugal pumps, investigation on design method with multi-operating conditions for nuclear pumps and research on mechanism of cavitation and its diagnoses, etc.

1 DESIGN METHODS FOR CENTRIFUGAL PUMPS

Aiming at the efficiency problem of centrifugal pumps, although much research has been done in China and other countries, a comprehensive research is still necessary because of the contradiction and intimate connection between the efficiency and brake horsepower characteristics of centrifugal pumps. A series of theoretical analysis and test research, aiming at the existing engineering problems and the frontier field, has been carried out by our research team, and a set of relatively improved hydraulic design methods for modern centrifugal pumps, especially for low specific speed centrifugal pumps, such as Greater Flow Design method, Non-Overload Theory and Splitter Blade Offset Design method, etc, is put forward. The achievements above, which have formed a specific system, are the development and improvement for the existing theory and hydraulic design method of centrifugal pumps, and have been applied by insiders in pump field.

1.1 Greater Flow Design[1]

The Greater Flow Design method is mainly for low specific speed centrifugal pump to improve its efficiency. The guiding principle behind the greater flow procedure is that, the given design flow and specific speed are increased, and then a larger pump is designed using increased flow rate and specific speed. As the efficiency curve η of larger pump almost covers that of the smaller one (reversed at lower flow) as shown in Figure 1, not only the best efficiency and design point efficiency, but also the average efficiency of the whole usage area will be improved.

1.1.1 Basic procedure of greater flow design

The basic procedure of greater flow design is that on the basis of a vast amount of tests the current design coefficients are revised in such a way that a compromise between flow and geometrical parameters is made for greater flow design suitable for low specific speed pumps. After that, reasonable flow combination and geometrical composition are designed considering revised parameters and integrative factors. The formulae are as follows:

$$Q' = K_Q Q \qquad n_s' = K_{ns} n_s \tag{1}$$

where Q and n_s represent design flow and specific speed respectively, Q' and n_s' represent magnified flow and specific speed respectively, and K_Q and K_{ns} represent magnification coefficients of flow and specific speed respectively, as listed in Table 1 and Table 2.

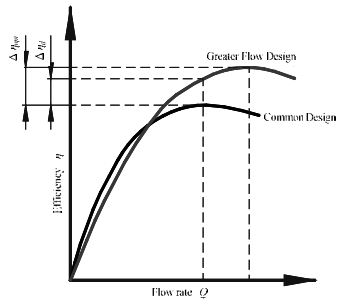

Figure 1 Principle of greater flow design

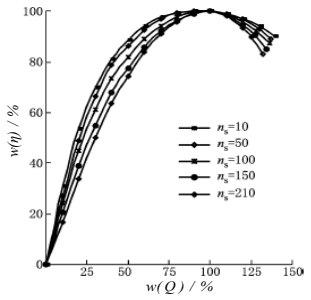

Figure 2 Dimensionless efficiency

Table 1 Magnification coefficient of flow K_Q

Q(m³/h)	3～6	7～10	11～15	16～20	21～25	26～30
K_Q	1.70	1.60	1.50	1.40	1.35	1.30

Table 2 Magnification coefficient of specific speed K_{ns}

n_s	23～30	31～40	41～50	51～60	61～70	71～80
K_{ns}	1.48	1.37	1.28	1.21	1.17	1.14

1.1.2 Optimization of enlarged factors

The closed constraint equations for solving magnification coefficients of flow and specific speed with obtaining the highest operation efficiency at the actual operating point as constraint was derived according to the principle of the enlarged flow design, and the valid numerical solutions are obtained[2], as shown in Figure 3. The broken line here represents the recommended values of magnification coefficients of specific speed in literature [1], and the optimized result is as basically same as actual one.

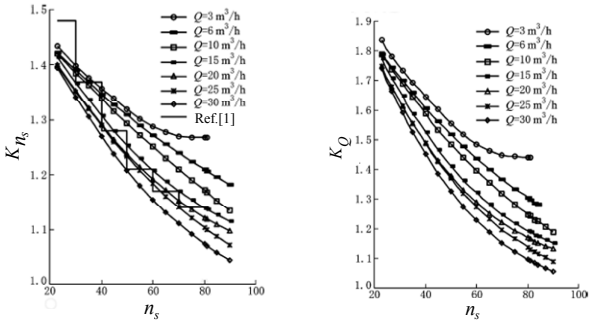

Figure 3 Relationships between n_s and K_Q, K_{ns} for various flow rates

1.2 Non-Overload Theory[1]

A non-overload centrifugal pump is referred to as the pump without overload or prime motor burning out by overload at any operating point in the range from shut-off head to zero head, and spare coefficient of pump brake horsepower K≈1.0 at design flow point. Its essence is to design a pump with a flat brake horsepower curve, which means the brake horsepower curve of centrifugal pump is a parabolic one with an extreme value, or the brake horsepower has small changes with flow increase. And that makes the brake horsepower less than or equal to the match power of prime motor at any operating point in the range from shut-off head to zero head (from zero flow rate to maximum flow).

The non-overload centrifugal submersible pumps have been widely used in agricultural irrigations and civil engineering. In order to know maximum brake horsepower and its location before the pump is manufactured, the author has derived the following prediction formulae:

$$P_{\max} = \frac{\rho}{4\eta_m} K_3 u_2^3 D_2 b_2 \psi_2 h_0^2 tg\beta_2$$
$$Q_{\max} = \frac{1}{2} K_4 h_o tg\beta_2 \eta_v \pi D_2 b_2 \psi_2 u_2 \quad (2)$$

where K_3, K_4 are correct coefficients for $P_{\max}$ and $Q_{\max}$ respectively, the author recommends here: K_3=1.0~1.1, K_4=1.05~1.15[1].

The restrained equations of non-overload pumps are also derived based on theoretical conditions of generation of saturation brake horsepower, and calculation formulae and relevant coefficients are revised considering synthetically the effect of geometrical parameters on pump operation performance. In addition, a set of design method and procedure for non-overload centrifugal pumps are put forward.

1.2.1 Restrained equations of non-overload pumps with low specific speed

$$\begin{cases} \Phi_{\max} = \dfrac{1}{2} h_0 tg\beta_2 \\ \dfrac{b_2}{D_2} = 0.0003752 n_s^{1.15} \qquad (20 < n_s < 80) \\ tg\beta_2 = \dfrac{n_s^{0.85}}{204 h_0 K_u^3} \\ 1.0 \le Y = \dfrac{\pi D_2 b_2 \psi_2 \sin\beta_2}{F_t} \le 2.0 \end{cases} \quad (3)$$

1.2.2 Design constants and procedure

Based on the restrained equations for specific speed n_s=30～80, the existing design coefficients for centrifugal pumps are appropriately revised, and the curve diagram suitable for design of non-overload centrifugal pumps is given. The procedure is as follows:

(1) Given design parameters (Q, H, n, η, P, etc), and calculate specific speed $n_s = \dfrac{3.65 n\sqrt{Q}}{H^{3/4}}$;

(2) Check Figure 4(a) to find out circumferential velocity coefficient of impeller K_u and b_2 / D_2, D_2 can be calculated from K_u, and b_2 can be worked out. Figure 4(b) shows dimensionless coefficient ψ and ω_s;

(3) Check Figure 4(c) to find out flow coefficient Φ and β_2, and make the Φ close to design point;

(4) Check Figure 4(d) to find out h_0;

(5) Select blade number Z, and commonly Z=4;

(6) Selection of other main geometrical parameters of impeller, vane drawing method, design of pump structure and design of pump casing or diffuser are all as same as ordinary design method;

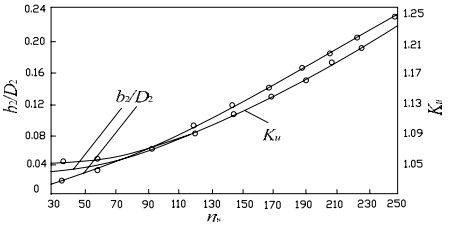

(a) Coefficients K_u and b_2 / D_2

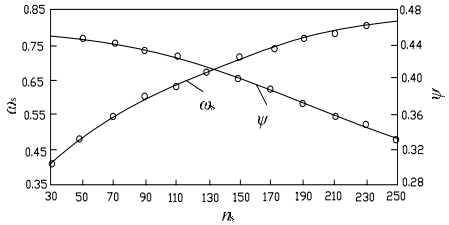

(b) Dimensionless coefficients ψ and ω_s

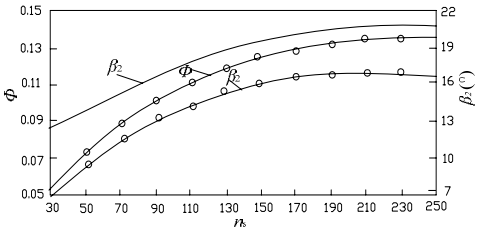

(c) Flow coefficients Φ and β_2

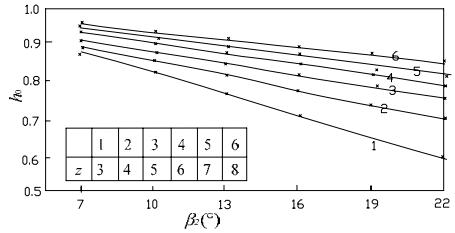

(d) Slip coefficient h_0

Figure 4 Coefficients of non-over load theory

(7) Each selected main geometrical parameter of impeller is substituted into the restrained equations and prediction formulae for P_{max} and Q_{max} to check calculation. If the results are not good, relevant parameters should be modified until satisfying results are obtained.

1.3 Splitter Blade Offset Technique [3]

The splitter-blade-offset design is one of the research focuses on low specific speed centrifugal pumps during the eighties of the twentieth century. Most of studies approved the effect of splitter blade on improving pumping head and efficiency of centrifugal pumps, and some guidelines and principles for design are given.

The optimal design of a low specific speed centrifugal pump with splitter blades is carried out by our research through two orthogonal tests, numerical simulation with multi-schemes and inner flow PIV measurement, and the rules of effect of splitter blade parameters on centrifugal pump performance are explored while main factors are found out.

Previous studies indicated that the splitter-blade-offset design has the following effects: ①effectively preventing the wake flow from generating and developing; ②washing away the wake flow; ③preventing the flow from separating on the suction surface and controlling the fluid movement effectively; ④increasing the slip factor for centrifugal impellers with the adding of splitter blades resulting in the increase in head or decrease in impeller diameter;⑤improving the velocity distribution within an impeller, reducing the hydraulic losses within an impeller and the mixed loss from impeller outlet to casing inlet and improving the pump performance. The design method for the low-specific speed centrifugal pumps with splitters, applicable to centrifugal pumps with specific speed below 80, is summarized through our investigating and using relevant achievements for reference.

1.3.1 Blade number *Z*

With the increase of blade number, the head increased, which is verified by our study; and through former studies, the schemes with 4 main blades have the best efficiency, so in general, considering the head and efficiency comprehensively, the blades number 4 is recommended.

1.3.2 Inlet diameter of splitters D_{si}

D_{si} has the direct bearing on the splitter length, and theoretically the longer are splitters (corresponding to smaller D_{si}), the higher is head of the pump. Test results show that, however, overlong splitter will cause the inlet blocking resulting in less increase of head and decrease of efficiency. With the splitter length decreasing, the structure of jet and wake cannot be improved, and the efficiency of pump cannot be increased. By statistics, for most low-specific speed centrifugal pumps, D_1/D_2=0.2~0.4, and combined with the principle of splitter length selection, $\alpha = 0.5 \sim 0.6$ when for larger value of D_1/D_2, the value of α adopts smaller one.

$$D_{si} = \left[\alpha(1 - \frac{D_1}{D_2}) + \frac{D_1}{D_2} \right] D_2 \tag{4}$$

Note: the formula and the value of coefficient α are just suitable for low specific centrifugal pumps with D_1/D_2=0.2~0.4.

In addition, a conclusion can be drawn from test results that the most excellent head and efficiency are obtained basically with the same inlet diameter splitter for impellers with different blade number.

1.3.3 Splitter deviating angle θ

Analyzing the inner flow of impeller through the flow slip theory, the velocity in impeller passage at the circumferential direction is not uniform, so the splitters cannot be set at the middle of flow passage, which need deviate to the main blades suction side to improve the flow structure of "jet-wake" and pump performance. Our studies show that, splitter deviation to the main blades suction side can improve pump performance, of which the effects on head and efficiency of pump are not obvious in certain range(1/5~1/6 blade channel width).

1.4 Design Method of Double Channel Pumps[4]

The research on non-clogging pumps used for environmental protection is currently focused on not only hydraulic design of single channel impeller, double channel impeller and volute, but also products development. Up to the present, no complete hydraulic design method of double channel pumps is available. Based on adequately knowing the structure of inner flow of double channel pumps, the impeller and volute design methods of double channel pumps are given by our team, particularly, not only the determination methods for channel midline of plane, but also the relationship between section ratio coefficient and specific speed are presented.

1.4.1 Impeller design method of double channel pumps

1. Mathematical modes of section of double channel impeller

(1) Representation of section of impeller and main geometrical parameters

The section of double channel impeller is shown in Figure 5, where D_j is inlet diameter of impeller, D_2 is outlet diameter,

b_2 is outlet width, R_1 is circle radius of shroud, R_2 is circle radius of hub, and T_1 and T_2 represent dip angles of shroud and hub respectively.

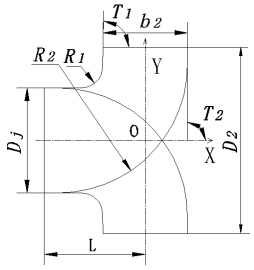

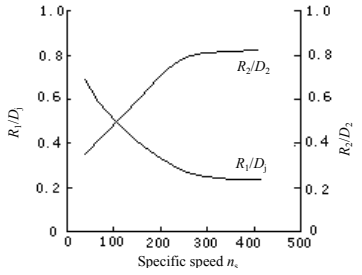

Figure 5 Section of the impeller Figure 6 Relation between n_s and R_1, R_2

(2) Calculation method of main geometrical parameters of section of impeller

(a) Though inlet diameter of impeller D_j, outlet diameter of impeller D_2 and outlet width of impeller b_2 are still calculated using classic speed coefficient method, more effects of two-phase flow on coefficient selection are considered.

(b) Circle radius of shroud and hub R_1, R_2

R_1 and R_2 can be represented as function relationships (n_s, D_j) and (n_s, D_2) respectively, and the calculating rules can be obtained by analyzing the statistics of large numbers of outstanding hydraulic models. In addition, R_1, R_2 can be determined by Figure 6 when design is being executed.

(c) Dip angles of shroud and hub T_1, T_2

Dip angle of shroud T_1 is approximately 87°, and dip angle of hub T_2 for most cases is 90°.

2. Mathematical models of plane of double channel impeller

(1) The rule of channel section area change

The channel midline section area changes according to linear law well when specific speed n_s is less than 150, and the area changes according to arc law when n_s is more than 150.

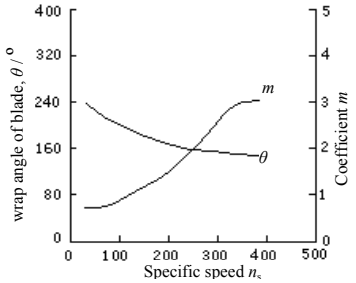

Figure 7 Relationships between n_s and φ, m

(2) Equation of channel midline oo′ of plane

It can be found that, result is excellent when a variant Archimedes Spiral is used, and the equation is as followed:

$$r = a\theta^m \tag{5}$$

where m represents a coefficient related to specific speed n_s, according to Figure 7

1.4.2 Volute design method of double channel pumps

(1) Though the calculation methods on base circle diameter D_3, inlet height b_3 and the tongue angle φ_0 are basically as same as methods for single phrase clear water, the value should be slightly bigger for non-clogging performance.

(2) Throat Area F_3

Throat area of volute F_3 can be obtained from area ratio coefficient y. By statistics, the relationship between y and n_s using least square method is as followed:

$$y = 0.1676 + 0.001030 n_s \tag{6}$$

1.5 Performance Prediction Methods [5]

Performance prediction for pumps is to predict the performance according to geometrical parameters of flow passage components (impeller, volute and diffuser, etc.), the pattern of inner flow and manufacturing accuracy, etc. Performance prediction, with advantages of improving design quality of products, shortening the period of product development and decreasing development cost, etc, is an important research subject of pump fields. The research on performance prediction for centrifugal pumps is carried out using hydraulic loss method, flow calculation method and neural network method respectively.

1.5.1 Hydraulic loss method

1. Hydraulic loss of impeller

Hydraulic loss of impeller is divided into impact loss of fluid inletΔh_1, friction loss of impeller channel Δh_2, diffusion loss of impeller Δh_3, hydraulic loss generated by fluid diverting Δh_4 and hydraulic loss of impeller outlet Δh_5. Relevant semi-empirical theoretical formulae are used for calculations respectively.

2. Hydraulic loss of volute

Hydraulic loss of volute is divided into friction loss Δh_1 and diffusion loss Δh_2, which are calculated by relevant semi-empirical theoretical formulae respectively.

3. Head prediction

Actual head of centrifugal pump H is equal to theoretical head H_t subtracting total hydraulic loss, which is shown as following

$$H = H_t - \sum \Delta h_i \tag{7}$$

where theoretical head is calculated by Stodola formula.

4. Efficiency prediction

Efficiency is predicted by following

$$\eta = \left(1/(\eta_v \eta_h) + \Delta P_d / P_e + 0.03\right)^{-1} \tag{8}$$

where volume efficiency η_v and disk friction loss ΔP_d are calculated by experiential formula respectively, while hydraulic efficiency is $\eta_h = H/H_t$, and hydraulic power is $P_e = \rho g Q H$.

1.5.2 Flow calculation method

Flow calculation method, whose essence is to establish the relationship between inner flow behavior and external performance of the pump, is based on results of flow calculation with CFD for performance prediction of pumps.

Without considering height of difference, the head of centrifugal pump H is

$$H = (P_{outlet} - P_{inlet}) / \rho g \tag{9}$$

where P_{outlet} is volute outlet total pressure, and P_{inlet} represents impeller inlet total pressure.

The prediction model of *NPSH* is

$$NPSH = (P_{T,inlet} - P_v)/(\rho g) \quad (10)$$

where $P_{T,inlet}$ is total pressure calculated from numerical result, P_v is evaporating pressure, ρ is density, and g is gravity acceleration.

1.5.3 Neural network method[6]

BP(Back-Propagated Delta Rule Networks) networks and RBF(Radial Basis Function Networks) networks are used to predict performance of centrifugal pumps.

1. Energy performance prediction

(1) Network input-output modes

Input modes: flow rate Q, impeller outlet diameter D_2, blade outlet width b_2, blade outlet angle β_2, blade wrap angle Φ, base circle diameter of volute D_3, volute inlet width b_3, the eighth cross section area of volute F_8 and blade number Z.

Output modes: head H and efficiency η.

(2) Network topological structure

The number of input layer neurons of BP networks and RBF networks can be determined as 9 according to input modes, and the number of output layer neurons is 2. For the determination of the number of hidden layer neurons, 20 neurons of BP networks are finally determined by comparison using trial-and-error method, and the structure of BP network finally is three layers structure 9-20-2, as shown in Figure 8. The number of radial base layer neurons of RBF network is equal to the number of iterations.

2. Cavitation performance prediction

(1) Network input-output modes

Input modes: flow rate Q, impeller inlet diameter D_j, blade inlet width b_1, curvature radius of impeller circle shroud R_1, blade incidence angle $\Delta\beta$, and blade number Z.

Output modes: net positive suction head $NPSH$.

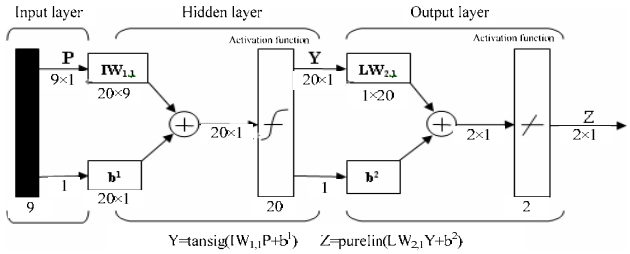

Figure 8 Structure of BP network

(2) Network topological structure

The number of input layer neurons of BP networks and RBF networks can be determined as 6 according to input modes, and the number of output layer neurons is 6. For the determination of the number of hidden layer neurons, 16 neurons of BP networks are finally determined by comparison using trial-and-error method, and the structure of BP network finally is three layers structure 6-16-1. The number of radial base layer neurons of RBF network is equal to the number of iterations.

1.6 Integrated CAD/CFD Software Development for Centrifugal Pumps[4,7-10]

Integrated CAD/CFD software includes hydraulic design, 3D modeling, performance prediction and CFD analysis, etc., and the correlation among all modules is shown in Figure 9.

1.6.1 Hydraulic design CAD software

Hydraulic design CAD software for centrifugal pumps is developed successfully based on secondary development of AutoCAD 2002 using VC++6.0 as the programming language. Three main modules are in the software including impeller, volute and diffuser design module.

1.6.2 Performance prediction software

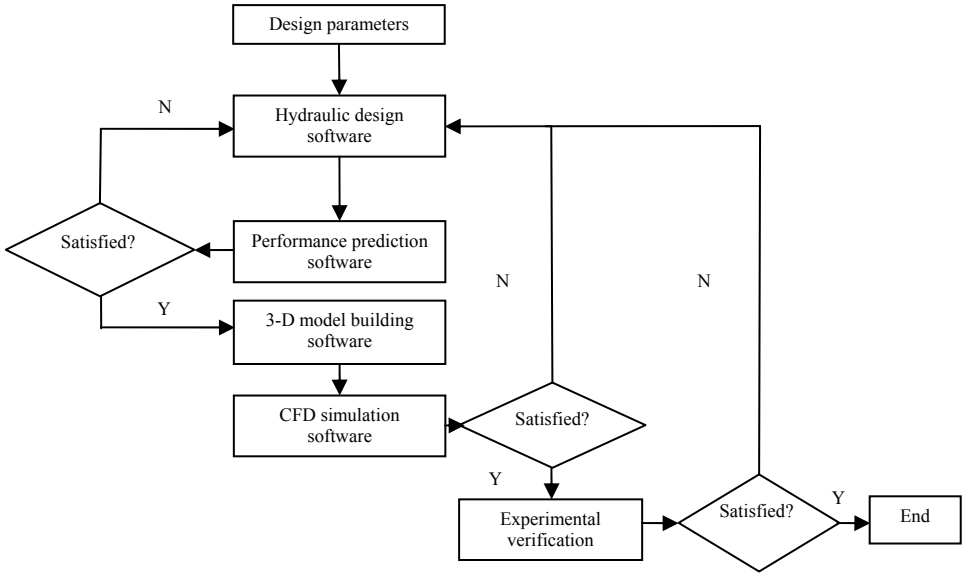

Figure 9 Relation graph of CAD/CFD software

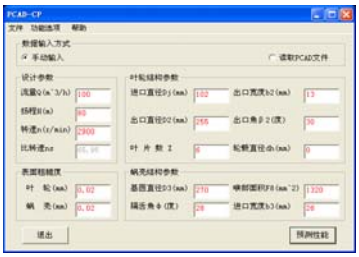

Figure 10 Dialog box of performance prediction software

Performance Prediction Software for Centrifugal Pumps has also been successfully developed based on secondary development of AutoCAD 2002 with hydraulic loss method using VC++6.0 as the language under ObjectARX 2000 environment. The software, consisting of input module, performance result module, loss calculation module, performance curve drawing module and curve modifying module, can draw out performance curve for centrifugal pumps directly. The dialog box is shown in Figure 10.

1.6.3 Parametric 3D modeling software

Parametric 3D Modeling Software for Centrifugal Pumps called PCAD-3D has been successfully developed based on secondary development of Pro/E using VC++6.0 as the language under Pro/TOOLKIT environment. Total five modules are in the software, including twisted blade module, cylindrical blade module, volute, double channel impeller module and radial diffuser module.

1.6.4 Automatic unstructured grid generating software

Automatic unstructured grid generating and optimizing software called PGrid, in which Optimization-Based smoothing is used for mesh optimization meanwhile Swapping technology and elimination of Sliver elements are taken into consideration, is developed combining AFT and Delaunay triangulation method. And relevant user interface form is developed using FLTK (Fast Light Tool Kit) for convenience.

1.6.5 Development of inner flow numerical simulation program

Numerical calculation program for solving Raynolds time-averaged Navier-Stokes equations, according to solution procedure of discrete governing equations, is compiled using FORTRAN language. The program, based on governing equations of flow and numerical method, is applicable for laminar or turbulent flow, compressible or incompressible flow and rotating or non-rotating flow. SIMPLEC algorithm and both standard $k-\varepsilon$ and $k-\varepsilon$ model considering rotation and curvature modification are supplied.

2 RESEARCH ON CHARACTERISTICS OF INNER FLOW FOR CENTRIFUGAL PUMPS

Both numerical simulations of unsteady turbulent flow and flow field measurements are carried out for multi-forms centrifugal pumps designed by various methods with same design parameters. The cavitation development can be estimated comprehensively according to characteristics of outlet pressure pulsation, the quasi-synchronous frequencies vibration and fractal dimension. In addition, FSI calculation using two-way coupling method is established for turbulent flow and vibrating structure to obtain the effect of fluid structure interaction.

2.1 Study on Characteristics of Inner Flow for Multi-Forms Centrifugal Pumps

2.1.1 PIV tests and numerical calculations for centrifugal pumps with splitters[3]

Two schemes of impellers were designed with three main blades and three splitters, and splitters inlet diameter is $0.7D_2$ when splitters relative long with $0.55L$of the main blades.

For the operational convenience of PIV and CCD systems, the model pump was designed with semi-volute inlet cavity to form axial inlet flow, and the impeller hub was transparent and perpendicular to the pump shaft; the impellers were shrouded and made of organic glass, which were transparent also; the outlet volte was made of stainless steel with several windows leaving for shooting laser and taking photos. The model pump and the PIV test rig are shown in Figure 11 and Figure 12 respectively, and more detailed information of impeller and volute can be obtained from Ref. [11]. The test results are shown in Figure 13.

Figure 11 Model pump

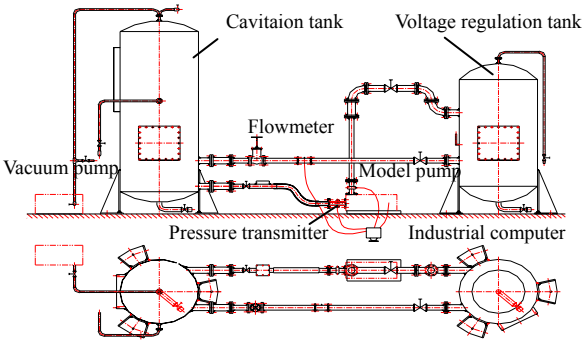

Figure 12 PIV test rig

1. PIV Test Results

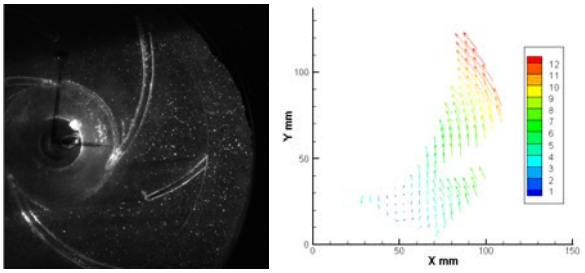

(a) Scheme 1

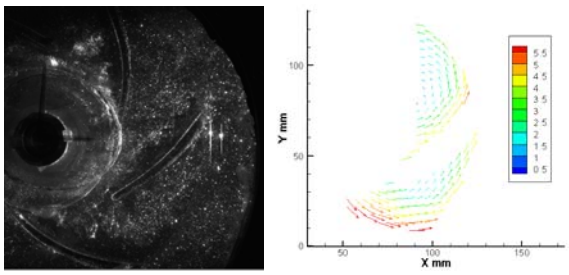

(b) Scheme 2

Figure 13 Relative velocity at 25m^3/h

2. Comparison with numerical simulation results

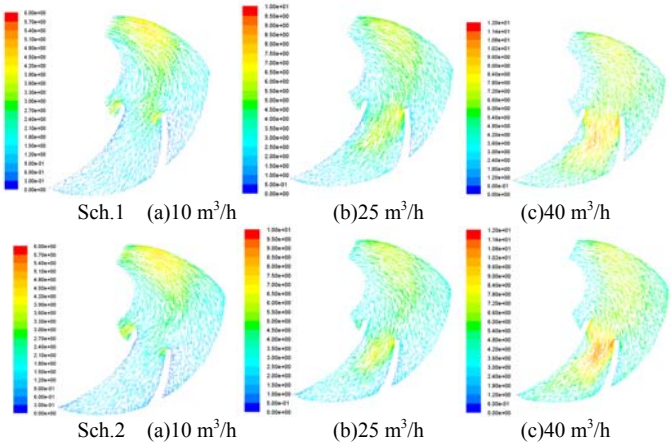

Sch.1 (a)10 m^3/h (b)25 m^3/h (c)40 m^3/h

Sch.2 (a)10 m^3/h (b)25 m^3/h (c)40 m^3/h

Figure 14 Relative velocity distributions at three typical flow rates

Five cases were selected for numerical simulations based on the PIV test. The RNG k-ε turbulent model was adopted to simulate the inner complex turbulent flow in five impellers at ten different flow rates. The relative velocity distributions on the mid section of impellers at three typical flow rates were shown in Figure 14. All these flow observations coincide with those from PIV measurement.

2.1.2 Unsteady simulations and comparison analysis for multi-design cases centrifugal pumps[12]

The problem of unstable inner flow always exists in low specific speed centrifugal pumps. Due to the pressure pulsations at outlet and inside the pump generated by unsteady flow, vibration and noise cannot stop being induced. In addition, characteristics of unsteady flow are different for various design cases of centrifugal pumps.

For comparing the unsteady characteristics of various design cases of low specific speed centrifugal pumps, the final five cases with same design parameters (Q =25m^3/h, H =10 m, n =1450 r/min), according to regular design method, low specific speed design method and splitter blade design method, were determined. Unsteady flow characteristics of different design cases were compared and analyzed with numerical calculation results.

1. Various design cases

(1)The first case is determined according to low specific speed design method[1], and main structure parameters include d_h=40mm, D_j=75mm, β_2=20°, D_2=188mm, b_2=12mm, Z=4, φ=160° and β_1=23.4°, as shown in Figure 15(a).

(2)The second case is determined according to velocity coefficient method[2], and main structure parameters are d_h=40mm, D_j=75mm, β_2=41°, D_2=180mm, b_2=9mm, Z=6, φ=80° and β_1=29.5°, as shown in Figure 15(b).

(3)For reducing severe crowding-out phenomenon at inlet of low specific speed centrifugal pumps, main blades and splitters are set normally with staggered arrangement.

The third case is the modification of the second, in which three non-neighboring main blades are replaced with splitters. The inlet diameter of splitters, without offset, is 0.7D_2. Hydraulic design is as shown in Figure 15(c).

(4)To study the effect of splitter offset on inner flow, the fourth case is the modification of the third, in which splitter offsets to the pressure side of main blade by 10°，as shown in Figure 15(d).

(5)To study the effect of splitter offset on inner flow, the fifth case is the modification of the third, in which splitter offsets to the suction side of main blade by 10°，as shown in Figure 15(e).

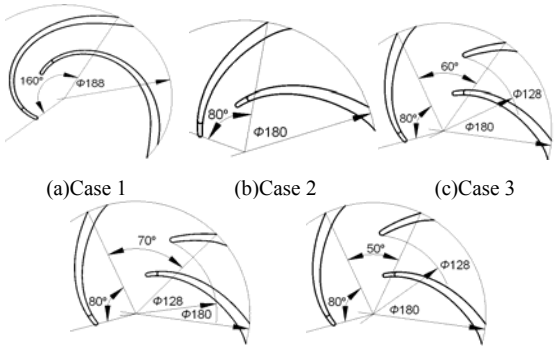

(a)Case 1 (b)Case 2 (c)Case 3

(d)Case 4 (e)Case 5

Figure 15 Impellers design draws based on different design principles

2. Models and methods of numerical calculation

The calculation domain is mainly composed of two parts, the static volute and the rotating impeller. The details for the unsteady calculations setting are shown in Ref. [12].

3. Main calculation results

Figure 16 shows the unsteady static pressure is much stronger in the area close to the tongue.

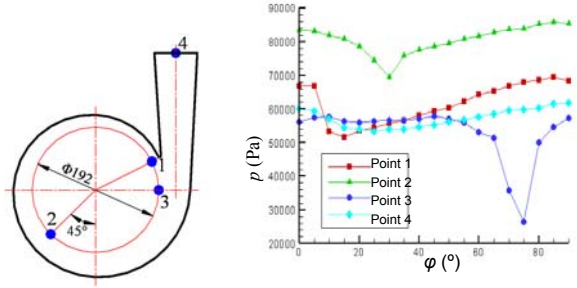

Figure 16 Static pressure at testing points in a period

Figure 17 shows static pressure fluctuations at four indicator points for various operation conditions. The impeller-

volute interaction has little effect on the result under partload condition, and especially the fluctuation can be hardly seen at the cross section of volute outlet.

Figure 18 shows the change of static pressure at point 1. The effect of different splitter offset directions on inner flow is totally different for the fifth case, in which splitter offsets to the suction side of main blade, has much smaller pressure fluctuation than the third and fourth case.

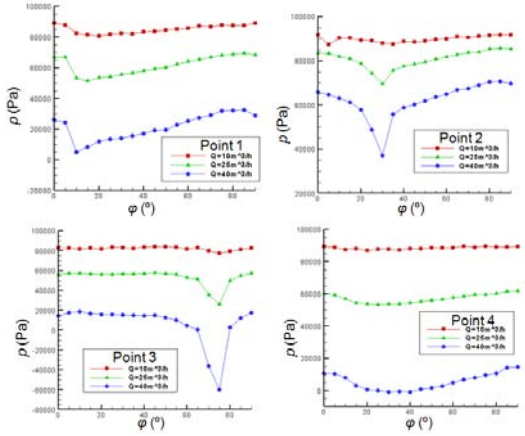

Figure 17 Static pressure at four testing points under different flow rates

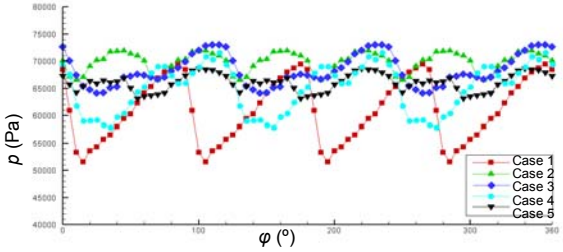

Figure 18 Static pressures at point 1 in a period under design condition

The unsteady flow caused by volute-impeller coupling interaction can result in the change of transient head of centrifugal pumps. The variation curves of head under different flow rate condition for five design cases are shown in Figure 19. The change amplitudes of transient head are reduced dramatically for various cases with decreasing of flow rate.

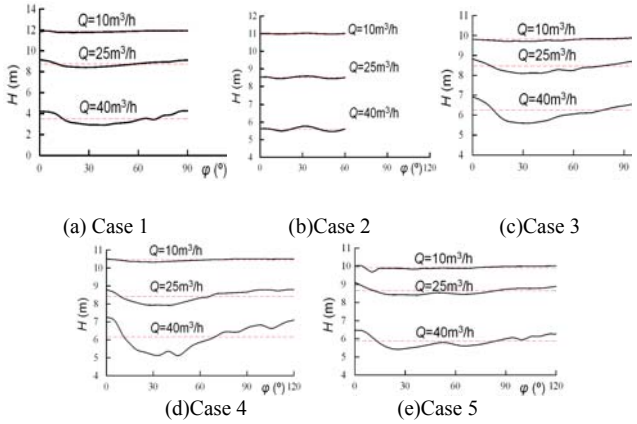

(a) Case 1 (b)Case 2 (c)Case 3

(d)Case 4 (e)Case 5

Figure 19 Instantaneous head of pumps under different flow rates

2.1.3 3D unsteady turbulent simulations [13]

Because of the three dimensional axial asymmetry configuration of the volute, the interaction between the impeller and the volute, i.e., the rotor-stator interaction inspires unsteady flow in pumps, and this interaction is an important effective factor of pressure pulsations in centrifugal pumps. The interaction between pressure pulsation and pump components not only is the main excited sources of vibration and noise in pump, but also can affect the flow around inlet and outlet of pumps.

The model pump is a low specific speed centrifugal pump designed by the greater flow design method (Q =12.5m^3/h, H =40 m, n =3500 r/min). The 3D unsteady turbulent simulation in full passage is carried out based on results from the steady calculations, and both the characteristic of pressure pulsation under design condition and inner flow variation of the pump under off-design conditions are analyzed. The characteristic of flow unsteadiness caused by impeller-volute interaction is primarily studied.

1. Design condition

Figure 20 shows the pressure fluctuation curves in time domain at the indicator points in impeller. Through analyzing the pressure fluctuation peak-to-peak values and dominant frequency, the pressure fluctuation is change more intensive from the inlet to the outlet of the impeller, which is alternating from 0.15 to 1.4 times of the local averaged pressure. The dominant frequency is 293Hz which is approximate to the blade passing frequency 291.7Hz.

Figure 21 is the pressure fluctuation curves in time domain at the points distributed in volute. The fluctuations have the identical features of five peaks and five valleys. The distribution feature of the static pressure in the casing is associated with its design.

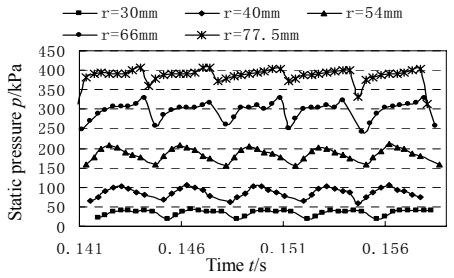

(a)Pressure side

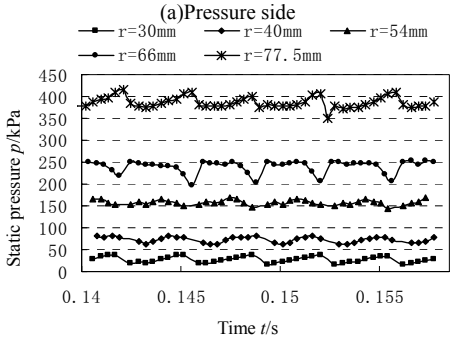

(b)Middle section

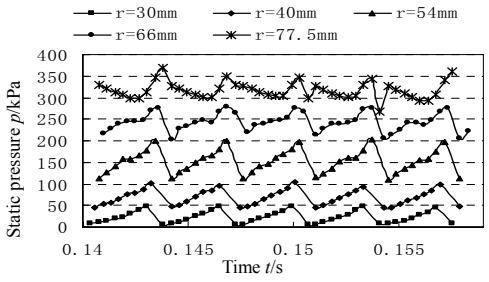

(c)Suction side

Figure 20 Pressure Fluctuation Curves of Points in Impeller

Figure 22 shows the frequency spectrum of pressure fluctuations in volute. No high frequency information occurs in casing. Because the casing is a collecting component, no new exciting component forces the flow.

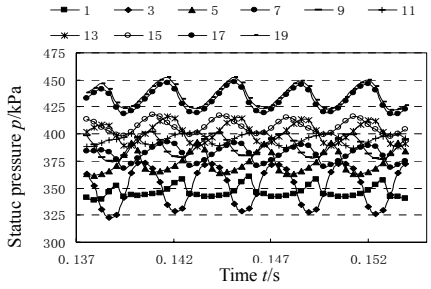

Figure 21 Pressure fluctuation curves of points in volute

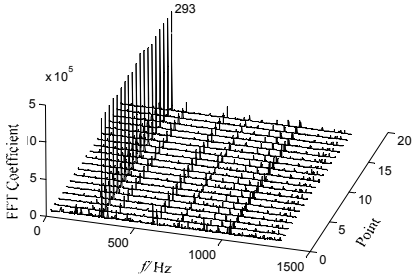

Figure 22 Frequency spectrums of pressure fluctuations in volute

2. Off-design condition

Figure 23 is pressure fluctuation curves in frequency domain at 19 points distributed in volute under off-design condition. High frequency fluctuations appear under low flow rate and high flow rate conditions, mainly because severe recirculation phenomenon exists in volute under the conditions.

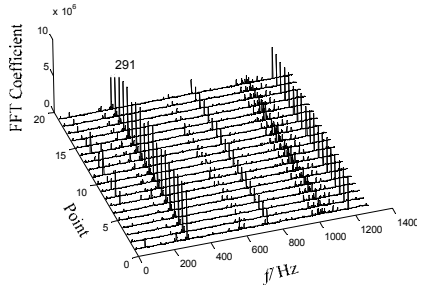

(a) Q=4.4 m^3/h

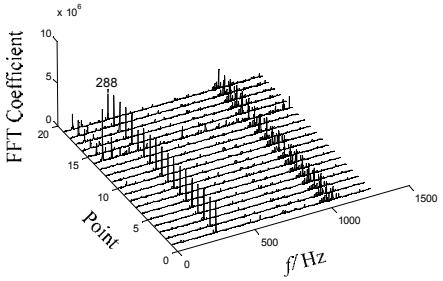

(b) Q=11.2 m^3/h

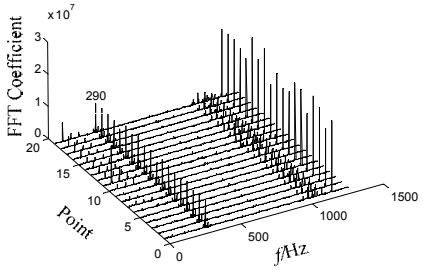

(c) Q=20 m^3/h

Figure 23 Pressure fluctuation curves in frequency domain

2.1.4 Numerical simulations and measurements for pressure fluctuations in double channel pumps[14,15]

1. Measurement of pressure fluctuations at volute outlet and inside double channel pump

(1)Pressure fluctuations at multi-positions in impeller and volute are studied by numerical method with sliding interface for double channel pump. Fluent software is used for the simulation, and clear water is used as medium. Pressure fluctuations at different-radius positions on midline of flow channel under design condition for a period are shown in Figure 24.

(2)The pressure fluctuation at the outlet of volute is measured using the underwater pressure sensors to join the Virtual Instrument system. Figure 25 shows pressure fluctuations in time domain for eight conditions. Figure 26 shows pressure fluctuations in frequency domain at the outlet of volute obtained by Fast Fourier Transform (FFT), where the ordinate represents amplitude of the fluctuation.

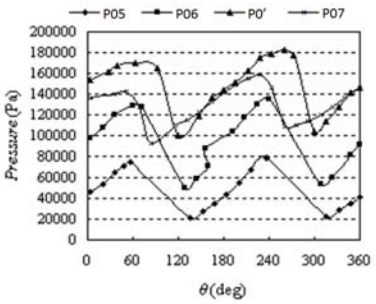

Figure 24 Pressure fluctuations in impeller passage

(3)Figure 27 shows the comparison between experimental and numerical results of pressure fluctuations at outlet of volute for one period. It presents that the average of the calculated

total pressure equals basically to what in the experiment. However, the pressure fluctuations of numerical calculation are smoother than the test while they both have the similar wave crest and hollow at the same time, which is approximate 0.01s. It can be concluded that there is a similar law of pressure fluctuation between numerical calculation and experiment.

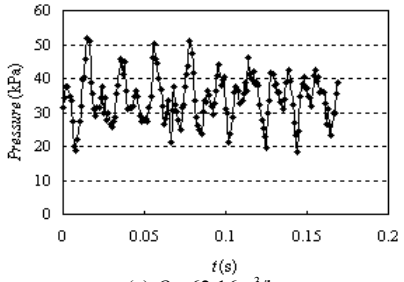

(a) Q_1=62.16m^3/h

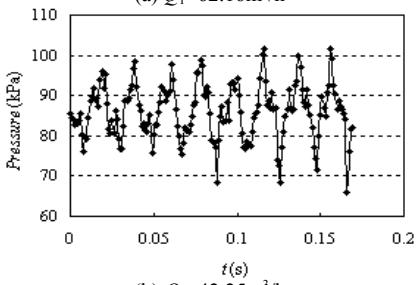

(b) Q_5=42.25m^3/h

Figure 25 Pressure fluctuations in time domain under eight conditions

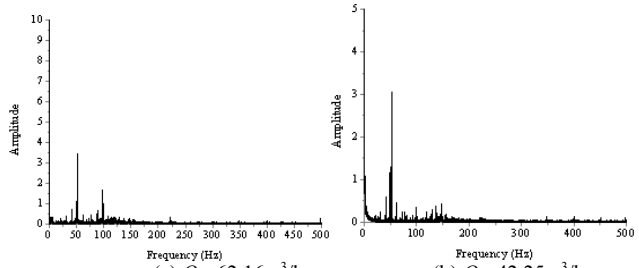

(a) Q_1=62.16m^3/h (b) Q_5=42.25m^3/h

Figure 26 Pressure fluctuations in frequency domain at the outlet of volute

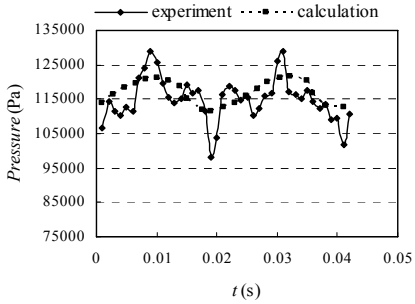

Figure 27 Comparisons between experimental and numerical results of pressure fluctuations at outlet of volute (Q_1=36.72m^3/h)

2. PIV measurement of inner flow in double channel pump

A number of measurement data are obtained to find out the velocity distribution law of inner flow using PIV measurement for double channel pump. The model pump is shown in Figure 28, and PIV equipment is shown in Figure 29. The laws of velocity vectors distributions are analyzed for different flow rates and rotating speeds, and the distributions of relative velocity vectors are obtained by Tecplot10, as shown in Figure 30.

Figure 28 Model pump Figure 29 PIV equipment

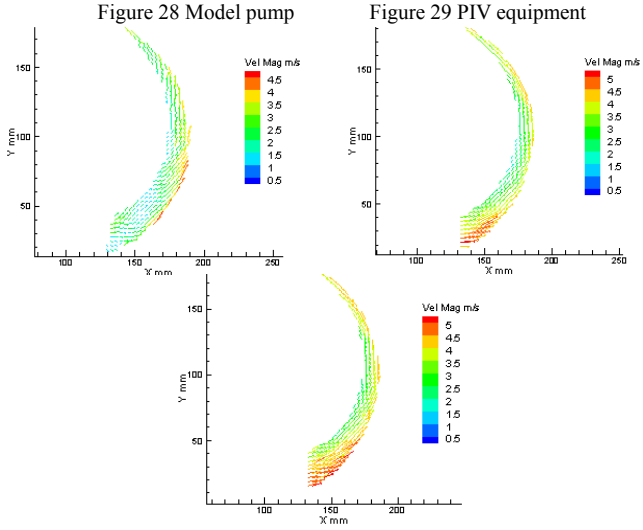

Figure 30 Distributions of relative velocity vectors

2.2 Research on Flow-Induced Noise and Vibration for Centrifugal Pumps

Flow-induced vibration in centrifugal pump is caused by cavitation, rotating stall, rotor-stator interaction and some other hydraulic excitations, which resulting in mechanical failure and noise. Therefore, the study, finding the inducement of vibration through inner flow analysis and experiment studies, is not only to maintain equipment and reduce environment noise but also to achieve the non-touch measurement of the interior flow in the pump.

2.2.1 Cavitation induced vibration and detection of cavitation[16]

Cavitation is a source of excitation which acts inside the main flow or adjacent to a solid wall. Hence, piezoelectric accelerate transducer which is mounted on the external wall for vibration and noise measurements can be used for detecting cavitation.

1. Vibration detecting method

The recycle loop is closed one, as shown in Figure 31. The loop consists of pressure tank, vacuum pump, pipeline system, valves, motor, pump and equipment for motor speed control, etc. FP203 pressure sensors are used for acquiring pressure data at inlet and outlet, and ultrasonic flow meter is used for flow rate measurement. Frequency convertor is used for changing rotating speed of motor which is acquired by speed

sensor. In addition, electric parameters of motor and vibration acceleration signals for each measuring point are necessarily measured.

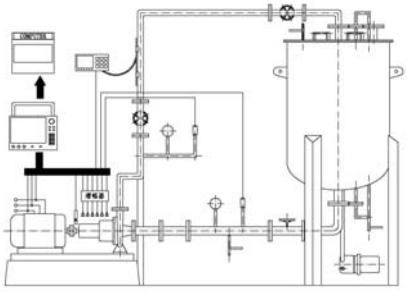

Figure 31 Recycle loop

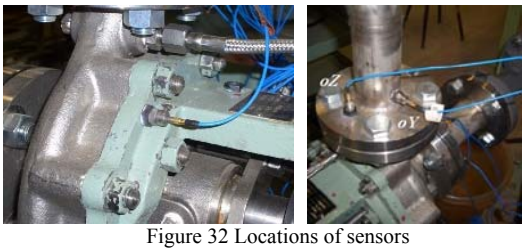

Figure 32 Locations of sensors

The vibration is measured by piezoelectric acceleration sensors MA352A60. Six sensors are mounted on the inlet, outlet, casing and the cover, respectively. The locations of sensors are shown in Figure 32.

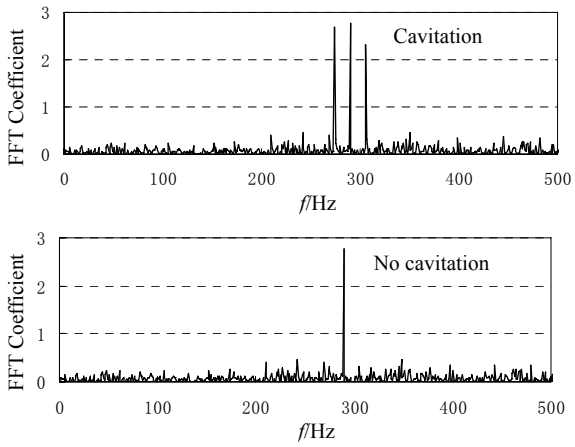

Figure 33 FFT results of both cavitation and non-cavitation conditions (Φ=0.30)

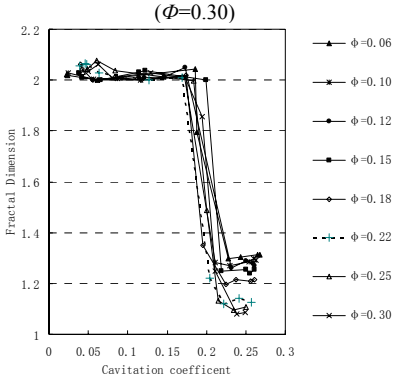

Figure 34 Fractural dimensions of the operation conditions

The vibration signals of both cavitation and non-cavitation are computed using an algorithm of Fast Fourier Transform (FFT). The prominent peak is at the blade passing frequency under non-cavitation situation. Two sub-peaks symmetrically appear on the two sides of the blade passing frequency on the condition of cavitation, while they are not discovered on the condition of non-cavitation, although the prominent peak is also at the blade passing frequency. The frequencies of the sub-peaks are called quasi-synchronous frequencies. Figure 33 shows the FFT results of both cavitation and non-cavitation conditions at the flow rate coefficient of 0.3. A same spectrum feature also appears at the flow rate coefficient of 0.10 and 0.22.

Figure 34 shows the fractural dimensions of the operation conditions via the flow the coefficient and the cavitation coefficient. It shows that the Higuchi fractal dimension is obviously correlated with the cavitation coefficient, but not with the operation conditions. With the variation of the cavitation coefficient, the fractal dimension is changing from 1.2 to 2.0. Before the incipiency of cavitation, the dimension is 1.2; along with the developing of the cavitation, the fractal dimension is increased correspondingly; when the cavitation is fully developed, the dimension is not increasing any more, and is around 2.0. Therefore, it is profound that the fractural dimensions are criterion which can describe the cavitation development.

2. Application for pressure pulsation of the pump outlet

Cavitation can cause pressure pulsations in the centrifugal pump. The pulsation is the essential property of cavitation, and is unrelated to time-average amount from measuring external characteristic. Therefore, the cavitation incipiency and developing procedure can be real-time monitored using the vibration signals.

The dimensionless pressure pulsation can be defined as

$$k_{p-p} = \frac{P_{puls}}{\overline{P}} \tag{11}$$

And absolute value of pressure fluctuation at outlet can be calculated by

$$P_{puls} = \sqrt{\frac{\sum_{i=1}^{N}\left(P_i - \overline{P}\right)^2}{N}} \tag{12}$$

where P_i represents transient pressure, N represents number of measurement and $\overline{P}$ represents time-averaged pressure at outlet.

The cavitation experiment under partload condition (22%Q) is described as the case to show the application of cavitation detection. The curve of cavitation development under 22%Q condition is shown in Figure 35. When cavitation has occurred slightly, favorable effects on performance of pumps exist for some time with *NPSHA* from 2.5m to 6.7m. Figure 36 shows the relationship between *NPSHA* and k_{p-p} under the situations in Figure 35. It can be seen that the value of k_{p-p} is no more than 5% and equals approximately 3.7% basically when *NPSHA* is bigger than 7.4m.

The value of $k_{p\text{-}p}$ is about 3.7% without cavitation occurring, and the value is close to 20% when cavitation has occurred strongly.

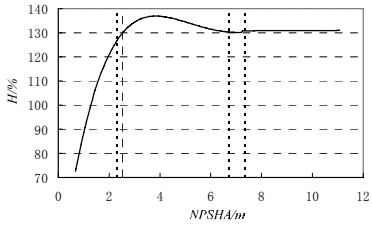

Figure 35 Curve of cavitation development under 22%Q

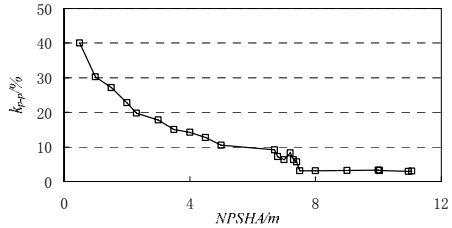

Figure 36 Relationship between *NPSHA* and $k_{p\text{-}p}$

The value of pressure pulsation of outlet, which is not stable and fluctuates between 5% and 9%, increases when *NPSHA* is from 6.7m to 7.4m. This is the stage of incipiency of cavitation, where feeble cavitation results in small but unstable pressure pulsations. When *NPSHA* begins to be less than 6.7m, the value increases regularly with the decrease of *NPSHA*, and quadratic parabola law is appeared. Corresponding to the point where head has decreased by 3%, the value of $k_{p\text{-}p}$ is close to 20%, and then the increase is faster. The characteristic of pressure fluctuations for other operation conditions has the relationship as similar as shown in Figure 36.

2.2.2 Analysis on characteristics of flow-induced vibration based on FSI method[17]

The interaction exists between complex inner flow and structures of centrifugal pumps. To gain the characteristics of vibration induced by hydrodynamic forces, both a solution of unsteady flow field and an analysis of the dynamic behavior of structure should be considered at one time. The FSI calculation of both pump inner flow and vibrating structure using two-way coupling method was established. The results, obtained by comparing flow fields calculated with and without FSI method were analyzed, and the deformation and stress of rotor calculated by FSI method were studied. Finally, the structural modal of rotor considering water pressure was studied.

1. FSI calculation and effect of rotor deformation on flow field

(1)FSI calculation process

Both pressure loads from the flow field acting on the structure and the impact of the impeller deformation on the flow field are taken into consideration, and the system uses iterative coupling where each physics field is solved sequentially. Two calculation domains, fluid calculation domain and structure calculation domain, are involved in the combined calculation for FSI effect of centrifugal pumps. Fluid solid interfaces are necessarily used on every fluid wetted impeller surface to establish an effective data transmission between fluid and structure field. The calculation models, which are achieved by Pro/E, are shown in Figure 37.

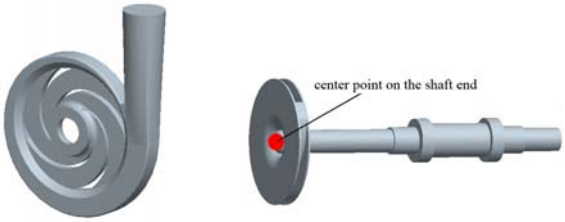

Figure 37 Sketch map of the pump model

(2)Effect of rotor deformation on flow field

To analyze the pressure distributions around outlet of impeller upon various positions relative to the cutwater and the changing trends with and without FSI, three time points are defined: t_1 for the point before blade passing cutwater, t_2 for the point of blade passing cutwater and t_3 for the point after blade passing cutwater. Figure 38 shows the comparisons of pressure distributions around outlet of impeller upon different positions relative to the cutwater under designed condition for the three time points. The FSI effect to the pressure distribution, of which the pattern is quite complicated, is not obvious relatively when the blade is passing cutwater.

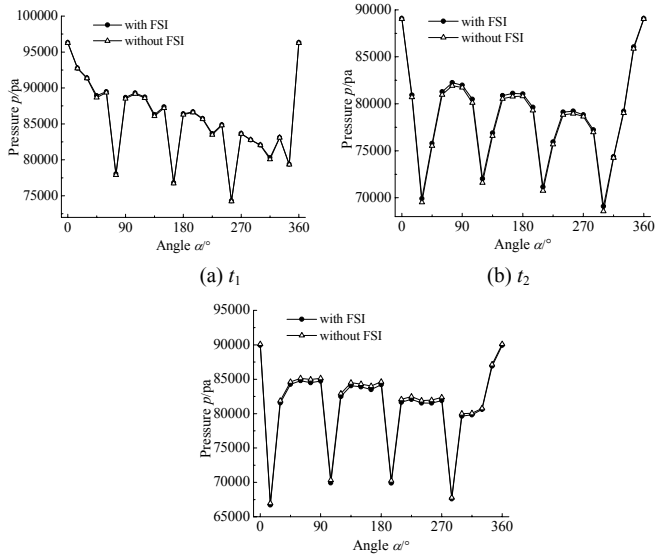

(a) t_1 (b) t_2

(c) t_3

Figure 38 Comparisons of pressure distributions around outlet of impeller with and without FSI

The pressure distributions on the tenth section of volute with and without FSI for the designated time point under 0.5Q conditions are shown in Figure 39. The changes exit for the results calculated with and without FSI. The effect of FSI, which is extremely complex, should be considered on studying pressure pulsations of inner flow in centrifugal pumps.

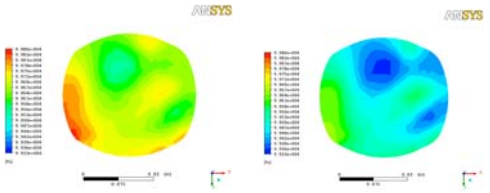

(a) with FSI (b) without FSI

Figure 39 Pressure distributions on the tenth section of volute

(3)Analysis of unsteady radial force

Amplitudes of radial forces time-dependent with and without FSI under 0.5Q conditions are shown in Figure 40, and every step represents the value of force amplitude for each time point calculated. Changing trends of peak values of radial force amplitude calculated with and without FSI are nearly same under high flow rate and design conditions while the peak value with FSI is slightly smaller than without FSI, and differently, the peak value with FSI is larger than without FSI under low flow rate.

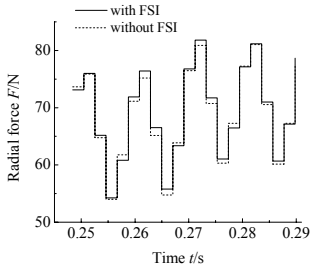

Figure 40 Amplitudes of radial forces with and without FSI under 0.5Q condition

The effect of FSI on the angle of radial force is quite complex, especially under 0.5Q condition. It is clear that some calculated angle values with FSI are evidently larger than without FSI, and some are smaller.

2. Analysis of structural dynamic characteristic of centrifugal pump based on FSI

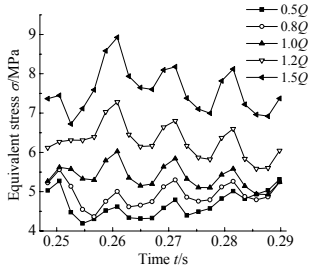

Figure 41 Fluctuations of equivalent stress with time for different operation conditions

Fluctuations of equivalent stress with time for different operation conditions are shown in Figure 41. The stress values change periodically and increase with the increase of flow rates. And the larger is flow rate, the more obvious is fluctuation.

Comparison of natural frequencies for first ten steps in two mediums is carried out. Vibration model of each order in air is similar to the one of same order in water though, nature frequency calculated in water is smaller than in air. The tenth order modal shape of the rotor is shown in Figure 42.

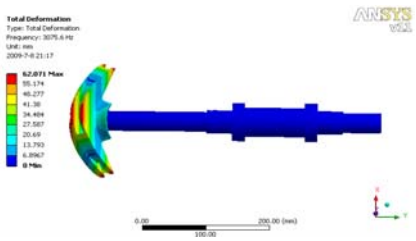

Figure 42 The 10th order modal shape of the rotor with water pressure

2.2.3 Numerical study on flow-induced noise for a centrifugal pump[18]

The flow-induced noise in a centrifugal pump is mainly caused by the unsteady flow inside a pump, which is a reaction form of inner flow in centrifugal pump. With the CFD software Fluent and the acoustic vibration analysis software SYSNOISE, a numerical study on the flow-induced noise of a centrifugal pump casing, based on FW-H equation, was carried out. Following the “acoustic analogy” method, the qualitative relationship between the background flow and the flow-induced noise was established. The study achievements will be the foundation for the further research of flow-induced noise and relevant engineering application.

Considering the completely rigid volute, the distributed dipole sources strength are determined by applying the boundary elements method (BEM), and the noise generated by the unsteady surface pressure fluctuation in the volute is predicted using SYSNIOSE. Figure 43 illustrates the dipole source strength.

There is a direct relationship between the surface distributed dipoles and the pressure fluctuation characteristics in volute. But the radiation effects of surface distributed dipoles at different frequencies would be different. To determine the amplitude of acoustic pressure field in the volute, considering magnitude of pressure pulsation is appropriate only for some special circumstances. The inhomogeneous wave equations are non-linear making that the relationship between the pressure pulsation and the dipole sources radiation characteristics is not a simple linear relationship. The forecast of acoustic pressure field considering other sources is also of great significance.

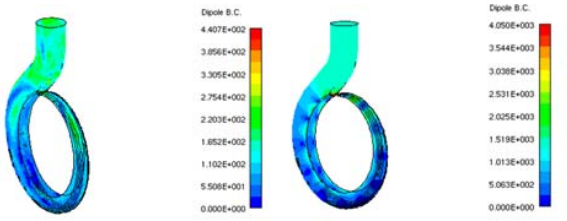

Figure 43 Dipole source strength distributions

4 FURTHER RESEARCHES

1. Research on design method

(1)CAD/CFD integrated software for centrifugal pumps should be carried out by self-compiling program.

(2)Design method of centrifugal pumps with low pressure pulsation, low vibration and low noise should be put forward through experiment research and inner flow analysis, etc.

(3)Establish an optimized hydraulic design method for multi-conditions of centrifugal pumps based on multidisciplinary design optimization method, and develop hydraulic models for multi-conditions operation by investigating inner flow pattern, finding the method of unstable flow control under off-design conditions and improving hydraulic design method for multi-conditions of centrifugal pumps.

2. Investigation on characteristics of inner flow

(1)Further investigate the generation mechanism and distribution law of unsteady flow phenomenon in centrifugal pumps based on precise numerical calculation and 3D PIV dynamic measurement.

(2)Further investigate the mechanism and spreading rules of noise and vibration induced by cavitation through measuring pressure pulsations, vibration and noise signals and inner flow field of cavitation.

(3)Further investigate the mechanism of various unsteady flow-induced vibration based on FSI calculation and vibration measurement.

(4)Further investigate the mechanism and spreading rules of various unsteady flow-induced noise based on acoustic vibration analysis and noise measurement.

ACKNOWLEDGMENTS

This project is supported by National Outstanding Young Scientists Founds of China (Grant No.50825902), Jiangsu Provincial Innovative Scholars "Climbing" Project of China (Grant No.BK2009006) and the Foundation for Senior Person with Ability in Jiangsu University of China (Grant No.08JDG040).

REFERENCES

[1] Yuan, S.Q., (1997) "The Theory and Design of Low Specific-Speed Centrifugal Pumps". Beijing: China Machine Press.

[2] Ni, Y.Y., Yuan, S.Q., Yuan, J.P., et al., (2008) "Model of Enlarged Flow Design for Low Specific Speed Centrifugal Pump". *Drainage and Irrigation Machinery*, 26(1), pp. 21-24.

[3] Yuan, S.Q. Zhang, J.F., Yuan, J.P., et al., (2009) "Research on the Design Method of the Centrifugal Pump with Splitter Blades". In Proceedings of the ASME Fluids Engineering Division Summer Meeting, August, Vail, Colorado USA.

[4] Liu, H.L., (2001) "The Research on CAD Software of Channel Non-clogging Pump and 3-D Incompressible Turbulent Flow in the Impeller". Zhenjiang, Jiangsu University. (In Chinese)

[5] Tan, M.G., Yuan, S.Q., Liu, H.L., et al., (2010) "Numerical Research on Performance Prediction for Centrifugal Pumps". *Chinese Journal of Mechanical Engineering. (English Edition)*, 23(1), pp. 21~26.

[6] Wang, Y., Liu, H.L., Yuan, S.Q., et al., (2009) "Prediction Research on Cavitation Performance for Centrifugal Pumps". In Proceedings of IEEE International Conference on Intelligent Computing and Intelligent Systems, November 20-22, Shanghai, China, (1), pp. 137~140.

[7] Zhao, B.J., (2008.) "3-D Numerical Simulation and PIV Measurement for Unsteady Turbulent Flow within Double-Channel Pumps". Zhenjiang, Jiangsu University. (In Chinese)

[8] Tan, M.G., (2008) "Prediction Research on Energy Characteristics for Centrifugal Pumps". Zhenjiang, Jiangsu University. (In Chinese)

[9] Liu, M., (2006) "Parametric Three Dimensional Modeling of Pumps and Its Software Development". Zhenjiang, Jiangsu University. (In Chinese)

[10] Lu, M.Z., (2009) "Investigation and Application of Tetrahedral Meshes Optimization Algorithms". Zhenjiang, Jiangsu University. (In Chinese)

[11] He, Y.S., (2005) "3-D Calculation of Turbulent Flow in the Centrifugal Pump Impeller with Splitting Vanes". Zhenjiang, Jiangsu University. (In Chinese)

[12] Yuan, J.P., (2009) "Inner Flow PIV Measurement and Its Unsteady Turbulent Flow Numerical Simulation for a Centrifugal Pump with Multi-Programs". Zhenjiang, Jiangsu University. (In Chinese)

[13] Ni, Y.Y., (2008) "3-D Unsteady Numerical Simulation and Fluid-induced Vibration for Centrifugal Pumps". Zhenjiang, Jiangsu University. (In Chinese)

[14] Liu, H.L., Lu, M.Z., Lu, B.B., et al., (2009) "Unsteady Flow Numerical Simulation in a Double Channel Pump and Measurements of Pressure Fluctuation at Volute Outlet". In Proceedings of the ASME 2009 Fluids Engineering Division Summer Meeting, August 2-6, Vail, Colorado USA.

[15] Lu, B.B., (2008) "Numerical Simulation of Flow in Double Channel Pumps and Measurements of Pressure Fluctuation". Zhenjiang, Jiangsu University. (In Chinese)

[16] Ni, Y.Y., Yuan, S.Q., Pan, Z.Y., et al., (2008) "Detection of Cavitation in Centrifugal Pump by Vibration Methods". *Chinese Journal of Mechanical Engineering. (English Edition)*, 21(5), pp. 46~49.

[17] Pei, J., (2009) "Numerical Study on Characteristics of Flow-induced Vibration for a Centrifugal Pump with FSI Method". Zhenjiang, Jiangsu University. (In Chinese)

[18] Xue, F., (2010) "Numerical Study on Flow-Induced Noise for a Centrifugal Pump". Zhenjiang, Jiangsu University. (In Chinese)

